# Collective Oscillations in Irreversible Coagulation Driven by Monomer Inputs and Large-Cluster Outputs

Robin C. Ball,[1,2] Colm Connaughton,[1,3,*] Peter P. Jones,[1] R. Rajesh,[4] and Oleg Zaboronski[3]

[1]*Centre for Complexity Science, University of Warwick, Gibbet Hill Road, Coventry CV4 7AL, United Kingdom*
[2]*Department of Physics, University of Warwick, Gibbet Hill Road, Coventry CV4 7AL, United Kingdom*
[3]*Mathematics Institute, University of Warwick, Gibbet Hill Road, Coventry CV4 7AL, United Kingdom*
[4]*Institute of Mathematical Sciences, CIT Campus, Taramani, Chennai 600113, India*

(Received 20 May 2012; published 17 October 2012)

We describe collective oscillatory behavior in the kinetics of irreversible coagulation with a constant input of monomers and removal of large clusters. For a broad class of collision rates, this system reaches a nonequilibrium stationary state at large times and the cluster size distribution tends to a universal form characterized by a constant flux of mass through the space of cluster sizes. Universality, in this context, means that the stationary state becomes independent of the cutoff as the cutoff grows. This universality is lost, however, if the aggregation rate between large and small clusters increases sufficiently steeply as a function of cluster sizes. We identify a transition to a regime in which the stationary state *vanishes* as the cutoff grows. This nonuniversal stationary state becomes unstable as the cutoff is increased. It undergoes a Hopf bifurcation after which the stationary state is replaced by persistent and periodic collective oscillations. These oscillations, which bear some similarities to relaxation oscillations in excitable media, carry pulses of mass through the space of cluster sizes such that the average mass flux through any cluster size remains constant. Universality is partially restored in the sense that the scaling of the period and amplitude of oscillation is inherited from the dynamical scaling exponents of the universal regime.

DOI: 10.1103/PhysRevLett.109.168304 PACS numbers: 82.40.Bj, 82.40.Ck, 83.80.Jx

The statistical dynamics of irreversible coagulation have been studied for almost a century since the pioneering work of Smoluchowski on Brownian coagulation of spherical droplets. See Ref. [1] for a modern review. It nevertheless remains an important branch of statistical physics. This is in part due to its status as a paradigm of nonequilibrium kinetics, but it is primarily due to its connections to a variety of important modern problems. We particularly highlight applications in cloud physics [2], surface growth [3], and planetary physics [4]. In these examples, coagulation of clusters is supplemented with a source (or effective source in the case of Ref. [4]) of small clusters or *monomers*. Such driven coagulation, in which monomers are supplied to the system at a constant rate, is the main focus of this Letter. One may expect the kinetics of such a system to become stationary for large times [5,6] with the loss of clusters due to coagulation compensated by the supply of new clusters provided by the input of monomers. In this Letter we show that this intuitive picture is not always correct and demonstrate the possibility of a new and strikingly different long-time behavior characterized by time-periodic kinetics.

Before we begin, let us introduce a large mass cutoff $\Lambda$. Above this size, clusters are removed from the system. Physically this could be literal removal as in the case of large droplets preferentially precipitating out of a cloud, or quenching of reactivity due, for example, to charge accumulation. Our primary motivation for introducing it, however, is theoretical, and we shall focus on what happens as $\Lambda \to \infty$. The basic quantity of interest is the cluster size distribution denoted by $N_m(t)$. It is the average density of clusters of mass $m$ at time $t$. Assuming that the system is statistically homogeneous, $N_m(t)$ has no spatial dependence. We denote the coagulation rate between clusters (or coagulation *kernel*) by $K(m_1, m_2)$. Suppressing the $t$ dependence of $N_m(t)$ for brevity, the mean-field kinetics satisfy Smoluchowski's equation:

$$\partial_t N_m = \frac{1}{2}\int_1^m dm_1 K(m_1, m-m_1) N_{m_1} N_{m-m_1} - N_m \int_1^{\Lambda-m} dm_1 K(m, m_1) N_{m_1} + J\delta(m-1) - L_m^{(\Lambda)}, \tag{1}$$

where $L_m^{(\Lambda)} = N_m \int_{\Lambda-m}^{\Lambda} dm_1 K(m, m_1) N_{m_1}$ removes clusters larger than $\Lambda$ and $J$ is the monomer injection rate. We study the family of kernels

$$K(m_1, m_2) = \frac{1}{2}(m_1^\nu m_2^\mu + m_1^\mu m_2^\nu), \tag{2}$$

which includes many of the commonly studied models [1]. Equation (2) can also capture the asymptotics of most physically relevant kernels. We mostly consider cases for which $\nu < 1$ and $\mu + \nu < 1$, avoiding complications due to gelation [1,7]. The stationary solution of Eq. (1) without cutoff was found in Ref. [8]. It is a power law for large $m$:

$$N_m = \sqrt{\frac{J[1-(\nu-\mu)^2]\cos[\pi(\nu-\mu)/2]}{4\pi}} m^{-(\nu+\mu+3)/2}. \tag{3}$$

 

The exponent $(\mu + \nu + 3)/2$ implies a constant flux $J$ of mass through each cluster size $m$. It is a standard example of a nonequilibrium stationary state with a conserved current. From Eq. (3), this stationary state exists only if $|\nu - \mu| < 1$, a fact which is true for any scale invariant kernel [9]. One might ask what happens if $|\nu - \mu| > 1$? This can occur in practice. Examples include coagulation of ice in planetary rings [4], gravitational clustering [10], and droplet sedimentation in static fluids [11].

The fact that the constant flux stationary state only exists for a certain class of kernels has long been appreciated in the theory of wave kinetics [12]. If one solves the stationary version of Eq. (1) with finite cutoff $\Lambda$ and studies the behavior as $\Lambda \to \infty$, one finds that when $|\nu - \mu| < 1$, the leading order term becomes independent of $\Lambda$. The stationary state thus tends to the universal form found in Ref. [8]. If, on the other hand, $|\nu - \mu| > 1$, the stationary state is nonuniversal and retains a dependence on $\Lambda$ as $\Lambda \to \infty$. This phenomenon is referred to as *nonlocality* of interaction (in the mass space) in the sense that all masses interact strongly with the largest or smallest masses in the system. By extension, the interactions in the regime $|\nu - \mu| < 1$ are termed *local* although this is a rather weak form of locality. A finite cutoff is essential to obtain a stationary state in the nonlocal regime as discussed in Ref. [13].

Almost nothing is presently known about the shape of $N_m$ in the nonlocal regime. We developed an algorithm to compute the exact stationary solution of the discrete version of Eq. (1) with cutoff by converting it into a two-dimensional minimization problem which can be easily solved numerically for modest values of $\Lambda$. For details see the Supplemental Material [14]. Some typical results are shown by the symbols in Fig. 1. It is clear that the nonlocal stationary state is not a simple power law. To obtain some analytic understanding, one possible way forward was outlined in Ref. [15]. If clusters of size $m$ grow primarily by interaction with clusters of mass $m_1 \ll m$, which is the essential feature of nonlocal interactions, one can Taylor expand the right-hand side of Eq. (1) and obtain an almost linear equation for $N_m(t)$ [15]. The dominant terms in this equation are

$$\frac{\partial N_m}{\partial t} = -D_{\mu+1}\frac{\partial}{\partial m}[m^\nu N_m] - D_\nu N_m, \tag{4}$$

where the $t$ dependence of $N_m$ has been suppressed and

$$D_{\mu+1} = \int_1^{m/2} m_1^{\mu+1} N_{m_1} dm_1 \to M_{\mu+1} = \int_1^{\Lambda} m_1^{\mu+1} N_{m_1} dm_1,$$

$$D_\nu = \int_m^{\Lambda} m_1^\nu N_{m_1} dm_1 \to M_\nu = \int_1^{\Lambda} m_1^\nu N_{m_1} dm_1.$$

Here we have introduced the notation $M_\alpha = \int_1^\Lambda m^\alpha N_m dm$, which will denote the $\alpha$ moment of the size distribution in what follows with $M_0$ and $M_1$ being the total number of clusters and total mass, respectively. Extension of the limits of integration of the above integrals to $\Lambda$ and 1, respectively, is a further assumption which needs to be justified *a posteriori*. The self-consistent calculation detailed in Ref. [16] for the case $\mu = 0$ is easily extended to obtain the following stationary asymptotic solution of Eq. (4) in the limit of large $M$:

$$N_m^* \sim \sqrt{2\gamma J \log(\Lambda)}\Lambda^{-1}\Lambda^{m^{-\gamma}} m^{-\nu}, \tag{5}$$

where $\gamma = \nu - \mu - 1$, adopting the convention that $\nu > \mu$ in Eq. (2). Detailed derivations of Eqs. (4) and (5) are provided in the Supplemental Material [14]. Equation (5) approximates well the true stationary state as indicated by the solid lines in Fig. 1. Note that there are no adjustable parameters. A striking feature of Eq. (5) is that the prefactor of the stationary state *vanishes* as $\Lambda \to \infty$, reflecting the nonuniversality of the nonlocal regime. Similar behavior was observed in the instantaneous gelation regime [17] in Ref. [16] although there is no gelation here.

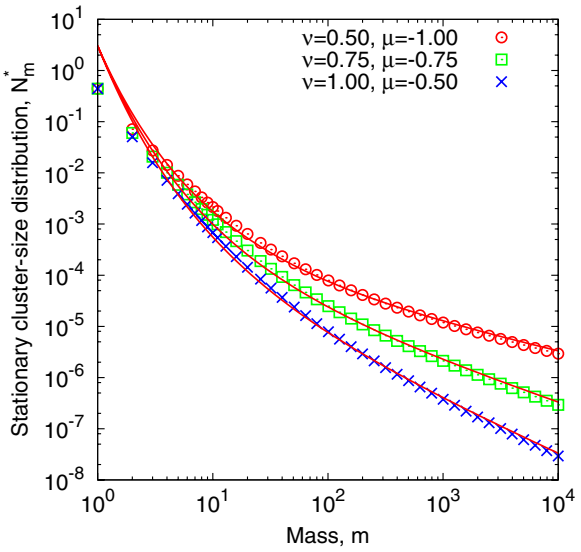


FIG. 1 (color online). Comparison of asymptotic approximation, Eq. (5) (solid lines), to the true stationary state of Eq. (1) obtained using our minimization algorithm (symbols). The kernels are given by Eq. (2) with values of $\nu$ and $\mu$ chosen in the nonlocal regime. The cutoff is $\Lambda = 10^4$.

The vanishing of the stationary state in the limit $\Lambda \to \infty$ poses a conceptual problem since it suggests the removal of the conduit linking the source to the sink. In order to investigate how the conserved mass current is carried in the nonlocal regime, we computed dynamical solutions of Eq. (1) in the nonlocal regime using the numerical algorithm developed in Ref. [18]. The results were surprising. For small values of $\Lambda$, the numerical solution converged to the exact stationary state as expected. Once $\Lambda$ exceeded a certain value, however, the numerical solution never reached the stationary state. The typical behavior of the total mass as a

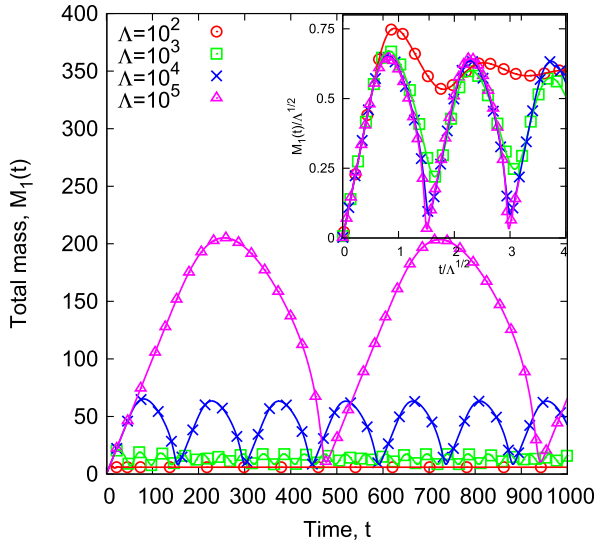


FIG. 2 (color online). Main panel: Total mass $M_1(t)$ versus time for different values of $\Lambda$ with $\nu = -\mu = \frac{3}{4}$. Inset: Collapse obtained by rescaling the data according to Eq. (8).

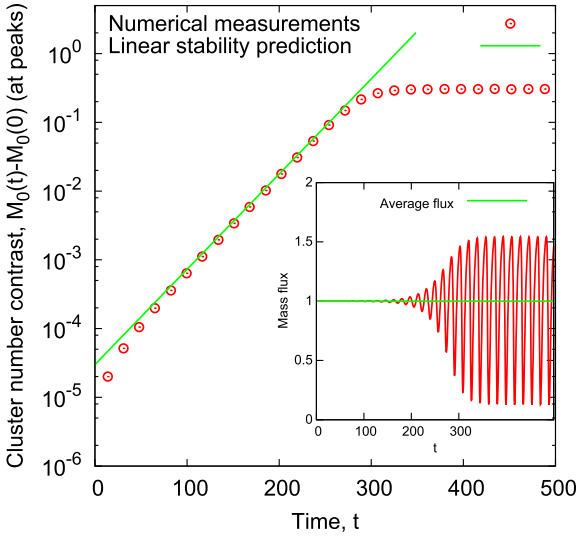


FIG. 3 (color online). Numerical evolution of a perturbation of the stationary state for $\nu = 1$, $\mu = -\frac{7}{8}$, and $\Lambda = 300$. Main panel: Amplitude of successive maxima of the perturbation (circles). The solid line is the prediction of linear stability analysis. Inset: The total output mass flux oscillates about its mean value of $J = 1$.

function of time for different values of $\Lambda$ is shown in the main panel of Fig. 2 for the case $\nu = -\mu = \frac{3}{4}$. Stationarity is reached only for smaller values of $\Lambda$. For larger $\Lambda$ we observe collective oscillations which seem to persist indefinitely (we stopped the computation after several hundred periods). The period and amplitude grow with $\Lambda$.

The intriguing possibility thus arises that the stationary state becomes unstable as $\Lambda$ increases. Our algorithm for computing the stationary state is not dynamical and makes no distinction between stable and unstable fixed points. We therefore input the exact stationary state as an initial condition for the dynamical code and added a small perturbation. The results for the density are shown in the inset of Fig. 3. The perturbation grows to a finite amplitude in a clear indication of instability. A lin-log plot of the amplitude of the successive maxima of the perturbation, as shown in the main panel of Fig. 3, indicates exponential growth, a clear sign of linear instability. We used MATHEMATICA to compute the eigenvalue $\zeta_{\max}$ of the linearization of the discrete version of Eq. (1) about the stationary state which has maximum real part. This analysis confirmed the instability. The growth rate agrees well with numerics (see the main panel of Fig. 3). For fixed $\nu$ and $\mu$, the stationary state undergoes a Hopf bifurcation as $\Lambda$ is increased. The eigenvalue $\zeta_{\max}$ crosses the imaginary axis at a critical value of $\Lambda$ (see the inset of Fig. 4), giving birth to a limit cycle and oscillatory behavior. The oscillations can be considered as a high-dimensional analogue of the relaxation oscillations observed in excitable systems such as the FitzHugh-Nagumo model of spike propagation in neurons [19]. Intuitively, these oscillations can be understood by noting that in the nonlocal regime, large clusters become very efficient at merging with small ones. As monomers are added to the system, the typical size remains fairly small until a small number of large clusters are generated. At this point, large clusters grow very rapidly by absorbing the smaller clusters producing a pulse of mass through the space of cluster sizes. These large clusters are then removed by the cutoff resetting the system to a state with almost no particles and the cycle repeats. The structure of the instability as a function of $\nu$ and $\mu$ for fixed $\Lambda$ is nontrivial, as shown in the main panel of Fig. 4. For fixed $\Lambda$, the stationary state becomes stable again for

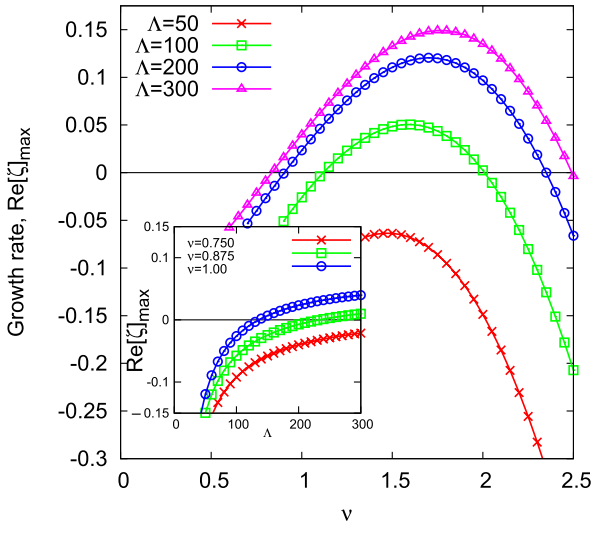


FIG. 4 (color online). Main panel: $\mathrm{Re}[\zeta]_{\max}$ for kernels $\mu = -\nu$ plotted as a function of $\nu$ for different values of the cutoff $\Lambda$. Inset: $\mathrm{Re}[\zeta]_{\max}$ as a function of $\Lambda$ for different values of $\nu$.

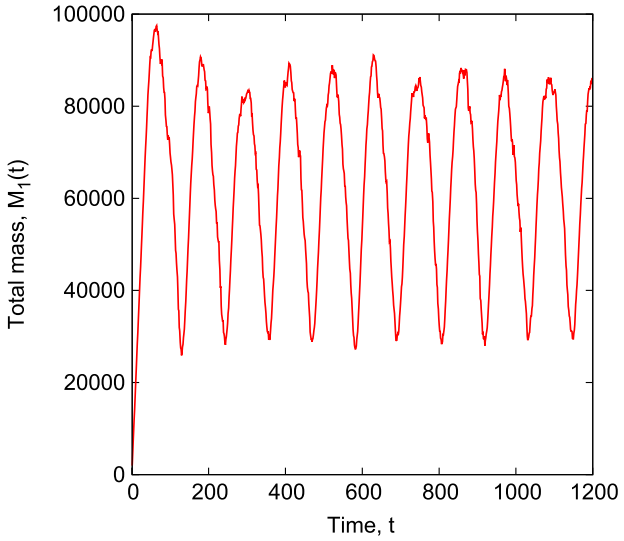


FIG. 5 (color online). Total mass versus time in a Monte Carlo simulation of the Markus-Lushnikov model with source and sink. Kernel is Eq. (2) with $\mu = -\nu = -0.95$ and $\Lambda = 300$.

sufficiently large values of $\nu$, a fact for which we have no intuitive explanation at present although we note that for $\nu > 1$ we are entering the instantaneous gelation regime where we would expect qualitative differences in behavior to appear [16]. Limit cycles appearing in mean-field equations can be destroyed by noise [20]. To check the robustness of this phenenomenon, we performed Monte Carlo simulations of the Markus-Lushnikov model (see Ref. [21]) with a source and sink of particles. Typical results are shown in Fig. 5. Oscillations are clearly visible, which remain coherent in the presence of noise.

To understand nonlinear aspects of the instability, such as the period and amplitude of nonlinear oscillation, we return to Eq. (1). Each period corresponds to a pulse of mass through the space of sizes (a movie is provided in the Supplemental Material [14]). Each pulse almost resets the mass of the system to zero as evident from the main panel of Fig. 2. Let us suppose each pulse grows with self-similar size distribution,

$$N_m(t) = s(t)^a F(\xi) \quad \text{with} \quad \xi = \frac{m}{s(t)}, \tag{6}$$

where $s(t)$ is a typical size and $a$ is an exponent to be determined. Substituting Eq. (6) into Eq. (1) and balancing dependences on $t$ requires that $\dot{s} = s^{\nu+\mu+a+2}$. Since the mass contained in each pulse grows linearly in time, $\int_0^\Lambda m N_m(t) dm = Jt$. Substituting Eq. (6) and differentiating gives $\dot{s} \sim s^{-a-1}$. Consistency requires

$$a = -\frac{\nu + \mu + 3}{2}, \qquad s(t) \sim t^{2/(1-\nu-\mu)}. \tag{7}$$

The period is estimated as the time $\tau_\Lambda$ required for the typical mass $s(t)$ to reach $\Lambda$. The amplitude $A_\Lambda$ is estimated as the mass supplied in one period. We thus obtain the following scalings for $\tau_\Lambda$ and $A_\Lambda$ with $\Lambda$:

$$\tau_\Lambda \sim \Lambda^{(1-\nu-\mu)/2}, \qquad A_\Lambda \sim J\Lambda^{(1-\nu-\mu)/2}. \tag{8}$$

These scalings are verified by the data collapse presented in the inset of Fig. 2. Universality is in a sense restored since the earlier universal behavior of Eq. (3) can now be understood as the special case in which $F(\xi)$ has the special form which cancels $s(t)$ from $N_m(t)$ in Eq. (6).

The phenomena presented here should be relevant beyond the idealized coagulation models analyzed above. The key requirement for oscillatory dynamics is nonlocality of the mass-space interactions, a concept which continues to make sense if, for example, the coagulation process is not scale invariant or is weakly reversible. Furthermore, many driven dissipative systems with conserved currents must satisfy a locality criterion analogous to the one discussed here Ref. [22] and may be candidates for oscillatory behavior when this criterion is violated. In particular, the kinetic equation for isotropic 3-wave turbulence, which is closely analogous to Eq. (1), becomes nonlocal when $|\nu - \mu| > 3$ [23]. Furthermore, the oscillatory behavior discussed in this Letter may even have been already observed experimentally in measurements of nonequilibrium phase separation of binary mixtures with slowly ramped temperature [24,25]. In this system, droplets of one phase coagulate inside another during demixing with nucleation providing the source of *monomers* although the coagulation process is not obviously nonlocal in our sense. This nevertheless seems like a potentially fruitful direction for further investigation since the theory presented here makes several testable predictions about the oscillatory kinetics.

C. C. thanks P. L. Krapivsky and E. M. Downes for enlightening discussions and acknowledges the support of the EPSRC (Grant No. EP/H051295/1) and the EU COST Action No. MP0806.

*connaughtonc@gmail.com

[1] F. Leyvraz, Phys. Rep. **383**, 95 (2003).
[2] G. Falkovich, A. Fouxon, and M. G. Stepanov, Nature (London) **419**, 151 (2002).
[3] Y. A. Kryukov and J. G. Amar, Phys. Rev. E **83**, 041611 (2011).
[4] N. V. Brilliantov, A. S. Bodrova, and P. L. Krapivsky, J. Stat. Mech. (2009) P06 011,.
[5] W. H. White, J. Colloid Interface Sci. **87**, 204 (1982).
[6] S. C. Davies, J. R. King, and J. A. D. Wattis, J. Phys. A **32**, 7745 (1999).
[7] E. M. Hendriks, M. H. Ernst, and R. M. Ziff, J. Stat. Phys. **31**, 519 (1983).
[8] H. Hayakawa, J. Phys. A **20**, L801 (1987).
[9] C. Connaughton, R. Rajesh, and O. Zaboronski, Phys. Rev. E **69**, 061114 (2004).

[10] V. Kontorovich, Physica (Amsterdam) **152–153D**, 676 (2001).
[11] H. Pruppacher and J. Klett, *Microphysics of Clouds and Precipitation* (Kluwer Academic, Dordrecht, Netherlands, 1997), 2nd ed.
[12] V. Zakharov, V. Lvov, and G. Falkovich, *Kolmogorov Spectra of Turbulence* (Springer-Verlag, Berlin, 1992).
[13] P. L. Krapivsky and C. Connaughton, J. Chem. Phys. **136**, 204 901 (2012).
[14] See Supplemental Material at http://link.aps.org/supplemental/10.1103/PhysRevLett.109.168304 for details of the derivations of Eqs. (4) and (5) in the main text and a movie showing the oscillatory behavior of the cluster size distribution.
[15] P. Horvai, S. V. Nazarenko, and T. H. M. Stein, J. Stat. Phys. **130**, 1177 (2008).
[16] R. C. Ball, C. Connaughton, T. H. M. Stein, and O. Zaboronski, Phys. Rev. E **84**, 011111 (2011).
[17] P. van Dongen, J. Phys. A **20**, 1889 (1987).
[18] M. Lee, Icarus **143**, 74 (2000); J. Phys. A **34**, 10 219 (2001).
[19] R. FitzHugh, Biophys. J. **1**, 445 (1961).
[20] M. Mobilia, J. Theor. Biol. **264**, 1 (2010).
[21] D. J. Aldous, Bernoulli **5**, 3 (1999).
[22] C. Connaughton, R. Rajesh, and O. Zaboronski, Phys. Rev. Lett. **98**, 080601 (2007).
[23] C. Connaughton, Physica (Amsterdam) **238D**, 2282 (2009).
[24] J. Vollmer, G. K. Auernhammer, and D. Vollmer, Phys. Rev. Lett. **98**, 115701 (2007).
[25] I. J. Benczik and J. Vollmer, Europhys. Lett. **91**, 36 003 (2010).